Investigation of Silver Diffusion in $TiO_2/Ag/TiO_2$ Coatings

J. Kulczyk-Malecka[1*], P. J. Kelly[1], G. West[1], G. C. B. Clarke[2], J. A. Ridealgh[3], K. P. Almtoft[4], A. L. Greer[5], Z. H. Barber[5]

[1]Surface Engineering Group, Manchester Metropolitan University, Chester Street, Manchester, M1 5GD, UK

[2]Pilkington United Kingdom Ltd., part of NSG Group, St Helens WA10 2RZ, UK

[3]Pilkington Technology Management Ltd., part of NSG Group, Lathom, L40 5UF, UK

[4]Danish Technological Institute, Tribology Centre, Build. 18, DK-8000 Aarhus C, Denmark

[5]Department of Materials Science & Metallurgy, University of Cambridge, 27 Charles Babbage Road, Cambridge CB3 0FS, UK

Abstract:

Low emissivity (low-*E*) coatings consisting of dielectric/silver/dielectric multi-layer stacks are applied to large-area architectural glazing to reduce heat losses from buildings. In this work $TiO_2/Ag/TiO_2$ stacks were deposited onto soda-lime glass by pulsed DC reactive magnetron sputtering. The coatings were annealed in the range 100−600ºC to study silver diffusion through neighbouring layers. Depth-profiling analysis was performed on these samples using time-of-flight secondary ion mass spectrometry and selected samples were also analysed by X-ray photoelectron spectroscopy and Rutherford backscattering spectrometry. Fick's second diffusion law

*Corresponding author: J.Kulczyk-Malecka@mmu.ac.uk
Tel: +441612476432

was used to find diffusion coefficient values and to investigate the temperature dependence of silver diffusion. To investigate film morphology and composition, scanning electron microscopy (SEM) and energy dispersive X-ray spectroscopy (EDX) were performed.

The purpose of this study is the requirement for the understanding of the issue of silver diffusion during annealing treatments used in glass fabrication and the results obtained show that silver diffuses through the adjacent layers in a stack during heat treatment. However, in the temperature range investigated, the diffusion rates did not follow n Arrhenius dependence. At higher temperatures and longer annealing times sodium also diffuses from the glass into the coating, replacing the silver between the titania layers.

Key words:

Magnetron sputtering; Diffusion; Low-*E* coatings; Titanium dioxide

*Corresponding author: J.Kulczyk-Malecka@mmu.ac.uk
Tel: +441612476432

1. Introduction

Sputtered silver-based coatings in multi-layer systems of dielectric/Ag/dielectric/glass and 'double silver' layer structures of dielectric/Ag/dielectric/Ag/dielectric/glass have excellent properties of heat insulation, solar energy reflection and low sheet resistance. At present, they are widely used as solar control coatings for automotive windscreens and electromagnetic-wave shielding coatings for plasma display panels and low emissivity (low-*E*) coatings [1, 2]. Among these applications, low-*E* coatings, which are applied to large-area architectural glazing to reduce heat losses from buildings, have the largest market [3]. They combine high visible transparency with high reflectance in the far-infrared region. To achieve this combination of properties, low-*E* coatings generally consist of dielectric/silver/dielectric multi-layer systems or stacks, where the thin (~10 nm) silver layer reflects long wavelength IR back into the building and the dielectric layers both protect the silver and act as anti-reflectance layers for visible light. The dielectric layers are commonly TiO_2, SnO_2 or ZnO [4], and all the layers are usually deposited by magnetron sputtering, which is considered to be one of the most important large-area coating technologies [3, 5]. However, the next generation of low-*E* coatings are increasingly deposited on toughenable glass, which is post-deposition annealed at temperatures of up to 650ºC. Under these conditions, silver atoms are highly mobile and can diffuse rapidly through the other constituent layers of the coating stack, which can have a detrimental impact on the performance of the coating [6]. Furthermore, sodium atoms may diffuse into the coating stack from the glass substrate. Titanium dioxide is a well characterised material and is widely used as a dielectric layer in low-*E* glass technology, which is why it was selected for this study. Depending on deposition conditions and post-deposition

*Corresponding author: J.Kulczyk-Malecka@mmu.ac.uk
Tel: +441612476432

processing, titania can, though, exist in three crystalline forms: anatase, rutile or brookite. As-deposited magnetron-sputtered TiO_2 is usually amorphous and transforms after annealing to anatase or rutile, or a mixture of phases, depending on the processing temperature [7-13].

Clearly, the structure and structural transformations in the titania dielectric layers may influence atomic diffusion through these layers.

The titania/Ag/titania stack in this work was chosen as a simple model for industrial-scale low-*E* coatings. After deposition, the samples were annealed in the range 100–600ºC for 5 minutes to investigate the temperature-dependent kinetics of silver diffusion. Diffusivity values, found by analysing the data according to Fick's second law, were used to determine activation energies and frequency factors from an Arrhenius plot.

2. Experimental methods

The titania/Ag/titania 'sandwich' stacks were deposited by magnetron sputtering onto 4 mm thick soda-lime glass and silicon wafer substrates. The titanium dioxide films were 80 nm thick, and were deposited prior to and following a 10 nm layer of silver. These stacks were deposited in a Teer Coatings UDP450 rig without breaking the vacuum by using a rotatable cylindrical drum as the substrate holder. The holder was positioned in the centre of the chamber, between two 300 mm×100 mm planar unbalanced magnetrons installed in the closed-field configuration [14]. This allowed the substrate to be held in front of each target in turn for the production of the stack. Titanium dioxide films were sputtered from a 99.5% purity metal target, driven by a dual channel Advanced Energy Pinnacle Plus power supply operating in pulsed DC

*Corresponding author: J.Kulczyk-Malecka@mmu.ac.uk
Tel: +441612476432

mode at an average power of 1 kW and a pulse frequency of 100 kHz and 5.0 μsec off time (i.e. 50% duty). An optical emission monitoring (OEM) system was used to control the amount of oxygen introduced into the system during the deposition of the titania films. The optimal conditions were found at an OEM signal of 20% of the full metal signal [15]. Silver coatings were sputtered in DC mode from a 99.9% purity metal target driven by the second channel of the Pinnacle Plus power supply at a power of 100 W. The chamber base pressure was in the range 5–6 × 10^{-4} Pa. To achieve an operating pressure of 0.3 Pa, 65 standard cubic centimetres per minute (SCCM) of argon were introduced into the chamber using an MKS mass-flow controller. The thicknesses of as-deposited titania samples were measured by profilometer (Dektak® 3, Veeco Instruments Inc.).

In addition, to investigate the variation of crystal structure of the titania layers during the annealing process, and the effect this might have on diffusion, a batch of titania-only coatings were deposited onto glass substrates under the same conditions to those used above. Raman (Renishaw inVia spectrometer with 514.4 nm wavelength argon ion laser) spectroscopy was carried out to determine the crystal structure of these titania coatings before and after annealing in air over a range of temperatures and times. To investigate surface morphology, the dielectric coatings were examined using scanning electron microscopy (SEM, Zeiss Supra 40VP) operating at 1–3 kV. Energy dispersive X-ray analysis with 40 mm^2 silicon drift detector (EDAX, Trident^{TM} system) with an electron beam energy of 8 keV was used to determine the stoichiometry of the deposited materials and to perform elemental mapping analysis across the surface of the samples.

After deposition, the stacks were annealed in the range 100–600^{o}C in air for 5 minutes and then a suite of analytical techniques was used to investigate the diffusion of

*Corresponding author: J.Kulczyk-Malecka@mmu.ac.uk
Tel: +441612476432

silver. This included time-of-flight secondary-ion mass spectrometry (TOF-SIMS) analysis (ION TOF 5) with a Bi_3^+ analysis beam and a 1 keV Cs^+ sputter beam, using a methodology explained elsewhere [6]. Due to the limited quantification of the TOF-SIMS results, selected samples were also analysed by X-ray photoelectron spectroscopy (XPS, VG-ESCALAB 220iXL spectrometer) and Rutherford backscattering spectrometry (RBS). In TOF-SIMS the intensity is given in arbitrary units that do not represent the real atomic concentration of silver in these samples. Nonetheless, this technique can indicate qualitatively how the silver profiles evolve at different annealing temperatures. XPS, on the other hand, measures atomic concentrations, enabling direct comparisons between samples. We would expect the silver concentration profile as a function of depth, after annealing, to show Gaussian broadening and reduced intensity with time (to maintain constant area). XPS depth-profiling was used to quantify the diffusion of silver and sodium. The pressure in the analysis chamber was typically 1.066×10^{-8} Pa and photoelectrons were collected from a 2 mm^2 sample area. An Al Kα monochromatic X-ray source was used with an argon ion gun, which bombarded the sample surface with energies of 1 keV at an incident angle of 45º. Ejected material travelled to the hemispherical sector analyser (HSA), where it was analysed.

The RBS measurements were carried out using 2 MeV $4He^+$ ions and a scattering angle of 161°. The detector measures the kinetic energy of the backscattered He ions. The energy of the backscattered He ions is dependent on the mass of the atoms they are scattered from and the depth at which the scattering event took place. The energy distributions were analysed using SIMNRA simulation software [16] and the SIM Target code [17].

*Corresponding author: J.Kulczyk-Malecka@mmu.ac.uk
Tel: +441612476432

3. Results and Discussion

3.1 Structure formation in titania coatings

Micro-Raman analysis was performed to investigate changes in the crystal structure of the titania coating after annealing. As mentioned above, titanium dioxide can form three main crystal structures: anatase (Pearson symbol *tI*12), rutile (*tP*6) and brookite (*oP*24) [18–19]. Analysis of anatase indicates the existence of 15 optical modes with the following representation of normal vibrations: $1A_{1g}+1A_{2u}+2B_{1g}+1B_{2u}+3E_g+2E_u$. Within this representation $1A_{1g}$, $2B_{1g}$, $3E_g$ are Raman active, whereas the remaining modes are active in the infrared [20].

Raman analysis gives information about the nature of the bonds in a structure, the position, shape and intensity of Raman peaks being related to sub-stoichiometric defects, quantum-confinement, crystal sizes, nanocrystallinity and large interfacial areas [8, 18–19, 21]. Spectra obtained from the titania films produced in this work were compared to those obtained from pure titania nano-crystals to allow variations in phase, stoichiometry or degree of crystallisation in the analysed films to be identified.

Figure 1 presents Raman spectra taken from an as-deposited coating, and coatings annealed at 200ºC or 400ºC for 10 minutes in air. The spectra from nanocrystalline rutile and anatase standards (Millennium Chemicals Ltd.) are also included in the figure. The spectra for all coatings may indicate short-range order (nanocrystallinity) in an amorphous matrix. The broad peak at 619 cm^{-1} may suggest a rutile structure, but the 450 cm^{-1} rutile peak is missing, suggesting that there is no long-range order in these samples. Indeed, it has been suggested that peak broadening occurs due to nanocrystallinity and quantum confinement effects, and that there is a

*Corresponding author: J.Kulczyk-Malecka@mmu.ac.uk
Tel: +441612476432

characteristic relation between grain size and peak position and broadening in Raman analysis [8, 19, 21–22]. Li Bassi *et al.* [18] pointed out that materials with smaller particles (~4.4 nm) have Raman spectra similar to those of amorphous materials.

Figure 2 presents the spectra for coatings annealed at 600°C for 10 or 30 minutes and 400°C for 30 minutes compared to anatase and rutile nanocrystalline powder standards. For all these samples, the spectra show clear evidence for the anatase structure (characteristic Raman shifts at 144, 399, 515 and 639 cm^{-1}). The strongest peaks are shown by the coating annealed at 400°C for 30 minutes. In contrast, the sample annealed at 600°C for 30 minutes shows a very weak peak at 400 cm^{-1}, suggesting that a long treatment at high temperature may cause degradation of the structure. Some peak broadening and shifting can also be seen, which could be caused by non-stoichiometric composition of the material or by small particle sizes [19].

The broad, weak peaks at about 1100 cm^{-1} arise from the glass substrate, as found by Xie *et al*. [23].

3.2 Diffusion behaviour in titania/Ag/titania stacks

Silver diffusion profiles for samples deposited on glass substrates and annealed in the range 100−600°C for 5 minutes were used to find diffusion coefficient values for Ag in these samples. Since the continuous thin layer of silver remains in the three-layer stack after the diffusion occurred under the annealing conditions investigated in this study, the diffusion equation (Fick's second law) was solved for an infinite couple with constant surface composition [4]. The solution for the concentration profile in this case is based on the error function [6, 24].

*Corresponding author: J.Kulczyk-Malecka@mmu.ac.uk
Tel: +441612476432

Diffusion coefficient values for silver atoms were calculated by curve fitting to an analytical solution of Fick's second law and finding the concentration of Ag by solving the complementary error function. Assuming that due to the different surroundings at the boundaries of each titania layer in the deposited stack, silver may diffuse with slightly different rates. The upper dielectric layer has an open surface and the lower dielectric layer has an interface with the substrate, which may change the diffusion kinetics quite significantly; therefore, both sides of the curve were fitted. Diffusivity values that combine the diffusion coefficients in both directions (towards the airside and glass substrate) are presented in Table 1. An Arrhenius plot is used to display the temperature dependence of the diffusion coefficient, D:

$$D=D_0 \exp(-Q/RT) \qquad (1)$$

where D_0 is the temperature-independent frequency factor, Q is the activation energy, R is the gas constant (8.314 J/mol.K) and T is the temperature in kelvin [25].

Figure 3 shows a gradual increase of diffusion coefficient values with annealing temperature; standard error bars are included in the graph. For stacks annealed at 100, 250 and 400^{o}C for 5 minutes the difference in silver diffusion coefficient values is rather insignificant, varying in the range of $3.5–5.8\times10^{-21}$ m^2/s. Only the stack annealed at 600^{o}C shows a diffusion rate one order of magnitude higher than the other samples. Therefore the linear trend expected from an Arrhenius plot was not obtained here. This may be related to the structural changes observed during annealing showed in figures 1 and 2. In general, silver diffusivity must be a function of temperature and of the structure of the phase through which it is diffusing, therefore two influences of the temperature needs to be considered. Firstly, increased temperature, while other parameters are being constant, would give a higher diffusivity. Secondly, increased

*Corresponding author: J.Kulczyk-Malecka@mmu.ac.uk
Tel: +441612476432

temperature in equal-time anneals, allows more structural relaxation, giving lower diffusivity. Since in this work the extent of increase the diffusivity with temperature is reduced, (i.e. the effective gradient and activation energy in the Arrhenius plot are reduced) it is possible that relaxation process strongly influences the diffusion, and therefore, non-linear plot has been obtained in figure 3.

It should be noted that these stacks were submitted to a constant annealing time of only 5 minutes (then the samples were removed from the oven and cooled in air). In other studies at higher temperatures, the annealing time was shortened to obtain a similar extent of diffusion in each heat treatment [26–28]. In the present study different annealing times were not investigated, and it appears that annealing below 600ºC results in little change in the silver diffusion rate as a function of temperature. It has, though, been pointed out by Mallard *et al.* that for diffusion coefficient values below 4×10^{-15} m^2/s, the data tend to be scattered and do not fit well to the Arrhenius equation [29]. This also may be the case here as silver diffusion coefficient values were in the range 10^{-20}–10^{-21} m^2/s. Such small diffusion extent, especially in samples annealed at lower temperature range, could imply that diffusion is related to the structure and interfacial roughness, not diffusion under annealing, meaning that presumable diffusion extent in as-deposited sample would be similar like these in samples annealed at lower temperatures. Therefore, there may also be change in diffusion as a function of time, which would relate to the film structure (i.e. silver is known to form islands not a continuous layer, see below), but it is not possible to separate these variables here.

To investigate the later stages of diffusion, a titania/silver/titania sample was annealed at 600ºC for one hour. This annealing time was selected to be long enough for the silver to diffuse completely through the titania, taking into account the silver layer

*Corresponding author: J.Kulczyk-Malecka@mmu.ac.uk
Tel: +441612476432

thickness and the modelled diffusion distances in samples annealed at the same temperature for 5 minutes. Figure 4 shows TOF-SIMS depth profiling analysis obtained from this sample. No silver peak was detected here, which supports the assumption that the silver is distributed throughout the titania layers. However, the silver intensity was expected to be much higher, considering the high sensitivity of the TOF-SIMS shown in figure 4. Such a low signal picked up from the silver suggests that either the silver layer is evenly distributed across the sample giving only a few counts at each sampling point or the silver has diffused into the glass and TOF-SIMS is picking up the trace remains of silver in the coating. Furthermore, it is interesting to note that sodium has replaced silver between the titania layers.

To measure the diffusion profiles in the titania/silver/titania stack quantitatively, samples annealed at 250^{o}C for 5 minutes and at 600^{o}C for 5 minutes and 1 hour were investigated by XPS. Since it was observed that sodium diffuses from the glass through the entire thickness of the coating stack after 1 hour annealing, additional samples were also deposited on silicon wafer substrates and annealed for 1 hour at 600^{o}C for comparison.

Figure 5 shows the distribution of silver in samples annealed at 250 and 600^{o}C for 5 minutes or 600^{o}C for 1 hour, deposited on glass and silicon wafer substrates. There are significant differences in the depth profiles of the samples deposited on different substrate materials. The stacks were all deposited during the same deposition run, therefore any potential run-to-run variations can be excluded here. This suggests that the differences in coatings structure and silver behaviour are related to the substrate material. In samples deposited on glass (black lines), only that annealed at 250^{o}C shows a silver peak, whereas the other samples apparently have almost no silver remaining in

*Corresponding author: J.Kulczyk-Malecka@mmu.ac.uk
Tel: +441612476432

the coatings. Comparing this with stacks deposited onto silicon wafers (grey lines), there is a discernible layer of silver present in each sample. For the stack annealed at 250ºC, the silver distribution has an approximately Gaussian shape. The areas under the silver curves for all the samples deposited on Si wafers show less than 5% difference between the samples annealed at 600ºC and the one annealed at 250ºC. Therefore silver is diffusing into the adjacent layers, but its presence can be still detected, unlike the coatings deposited onto glass substrates, where XPS picked up negligible signals from silver. Similar silver profiles are observed from both TOF-SIMS (Fig. 4) and XPS analysis (Fig. 5) for the sample deposited onto a glass substrate and annealed at 600ºC for one hour. This suggests that silver diffuses into the glass substrate during longer annealing times at a relatively high temperature. On the other hand, there is a relatively strong signal picked up from the sample annealed at 600ºC for 5 minutes and analysed by TOF-SIMS, whereas XPS failed to detect any silver. The authors believe that this is related to the higher sensitivity of the TOF-SIMS technique [30–32].

Figure 6 shows SEM micrographs of the surface morphology of the TiO_2/Ag/TiO_2 samples deposited on glass and Si wafer and annealed at 250ºC or 600ºC. In most of the samples, due to the diffusion through the top layer, silver atoms have agglomerated on the film surface, creating clusters. The compositional contrast given by the backscatter detector gives a clear distribution of grains on the sample surface. Silver particles are brighter as they have the highest density in the analysed titania/silver/titania stack. However, the sample deposited onto a glass substrate and annealed at 600ºC for 1 hour (figure 6 b) shows much less silver clustering on the surface. There are still white spots present, which are probably Ag, but the characteristic larger clusters cannot be seen. This may be related to silver diffusion into the glass

*Corresponding author: J.Kulczyk-Malecka@mmu.ac.uk
Tel: +441612476432

substrate or a very thin silver layer spreading evenly on the surface, rather than creating clusters.

To confirm that the white areas detected by SEM analysis are really silver clusters, EDX mapping was performed. Figure 7 shows atomic distributions on the surface of the sample deposited onto silicon and annealed at 600^{o}C for 1 hour. Comparing the silver map with the SEM image it is clearly seen that the bright areas are silver agglomerations on the coating surface. However the mapping analysis could not be performed on the sample deposited onto the glass substrate and annealed at 600^{o}C for 1 hour, due to the sensitivity limitations of the instrument used: the silver concentration was too low at the sample surface to distinguish it from other elements.

EDX compositional analysis was also performed to find the atomic composition of the titania/silver/titania samples. Tables 2 and 3 show the composition of the titania/silver/titania stacks deposited onto silicon and glass substrates, respectively, and annealed at 600^{o}C for 1 hour. The atomic concentration of silver in the sample deposited onto glass is about 3% less than in the sample deposited onto silicon. This suggests that instead of creating cluster agglomerations on the film surface, silver probably diffuses into the glass substrate. The EDX ion beam penetrates the samples to a depth of about 1 µm. Considering that the stack is only about 170 nm thick, the remaining signal must come from the glass substrate. The concentration of silver is still extremely low in samples deposited on glass, in comparison to those deposited on silicon. This suggests that silver atoms have penetrated the glass to a depth greater than 1 µm. A similar process to ion-exchange diffusion might have occurred between Na and Ag over longer annealing time at relatively high temperature, as shown in figure 4. Silver-doped glass has applications in optoelectronics, colour changing in decorative

*Corresponding author: J.Kulczyk-Malecka@mmu.ac.uk
Tel: +441612476432

glasses and in hybrid microelectronics as interconnections or electrodes for dielectric layers [33–35]. It has been reported by Sheng *et al*. that for thermal treatments at temperatures above 320^{o}C and an annealing time of 1 hour, an ion-exchange process took place and silver diffused into the glass matrix replacing alkaline ions present on the glass surface, which supports our hypothesis [33]. It was reported elsewhere that after annealing at 600^{o}C for 45 hours the depth reached by silver was more than 200 µm [34], therefore it might be expected that silver could have reached a depth greater than 1 µm in the glass matrix in the samples analysed here.

To test the ion-exchange diffusion hypothesis, an as-deposited sample and samples annealed at 250^{o}C for 5 minutes and at 600^{o}C for 1 hour were analysed by RBS. Figure 8 shows the measured RBS data and a simulated profile collected from an as-deposited titania/Ag/titania sample on glass, whereas Figure 9 shows the measured data and a simulated profile for the same sample annealed at 600^{o}C for 1 hour. The *x*–axis refers to the kinetic energy of the backscattered He ions. While it is possible to extract a depth concentration profile for the various elements from such data, it is necessary to know the approximate structure of the layered coating and the nature of the substrate. The *y*–axis on the RBS spectra is the number of backscattered He ions (with a certain kinetic energy). Since the number of backscattered ions from an element is proportional to the concentration weighted by the scattering cross section ($\sim Z^2$), the concentration of an element at a certain depth can be extracted from the data. For heavier elements the scattering cross sections are higher.

The various contributions to the simulated profile from different elements are shown individually in the following figures. In Figure 10 the compositional depth profiles extracted from the simulation are shown for the as-deposited titania/Ag/titania

*Corresponding author: J.Kulczyk-Malecka@mmu.ac.uk
Tel: +441612476432

stacks. If the atomic density (at/cm^3) of the material is known, the depth can be converted to nanometres by dividing the RBS depth with the atomic density. The concentration of Ag in the annealed sample is very low due to diffusion and can only be seen when the appropriate concentration values are magnified. Figure 11 allows a direct comparison of the concentration profiles for silver in the as-deposited and annealed titania/Ag/titania samples.

RBS measurements showed that fairly good agreement between the measured data and the simulations was obtained in both the as-deposited and annealed titania/Ag/titania samples using the models chosen for the compositional profile. The peak at about 1400 keV in figures 8 and 9 refers to Ti from TiO_2. If the TiO_2 layer has a homogeneous concentration profile, the height of the measured signal from TiO_2 should be almost flat. The 'dip' in the peak reveals that the Ag layer is sandwiched between two TiO_2 layers. The dip in the Ti counts corresponds to a local region with less Ti than the surrounding part of the coating. This dip should in principle also be visible in the O signal, but since the scattering cross section of O is much lower, a significant concentration change is needed in order to detect the change. Typically, the O concentration should change by about 10 at.% in order to really see this effect and, furthermore, since the O signal is added on top of signals from other elements this makes a relative change for O even more difficult to observe.

On the other hand, if Ag was present on the surface of the as-deposited sample its signal should rise at an energy of ~1730 keV. However, the main Ag signal in the TiO_2/Ag/TiO_2 samples rose at a lower energy (the main part of the silver signal is found between 1660–1690 keV due to the energy loss of He ions when traversing through the primarily TiO_2 layer), which means it is present at some depth below the film surface.

*Corresponding author: J.Kulczyk-Malecka@mmu.ac.uk
Tel: +441612476432

Silver in the as-deposited sample shows one peak, indicating a single layer (see figure 8). The shoulder on the high energy side may suggest a small Ag tail towards the substrate surface. In the as-deposited sample the Ag layer is mainly located between the two TiO_2 layers, but it is not separated from the TiO_2 layers by sharp interfaces, which might be due to either mixing by diffusion or due to island growth of the Ag. As Ag is commonly known to exhibit island growth this might lead to a less well-defined layer. The atomic density of bulk Ag is ~ 5.8×10^{22} at/cm^3 [36]. This means that e.g. a pure Ag layer of 10 nm corresponds to a 'thickness' of 10^{-6} cm$\times5.8\times10^{22}$ at/cm^3, which equals 58×10^{15} at/cm^2. The FWHM of the simulated Ag peak is 40×10^{15} at/cm^2, which would approximate to a layer thickness of 7 nm at bulk density. Thus, the observed Ag signal cannot be simulated by a pure Ag layer 10 nm thick. The implication is that either the layer thickness is indeed less than expected or, more likely, some mixing between the adjacent layers has occurred and the resulting coating density is lower than the bulk value for silver (a value of 4×10^{22} at/cm^3 can be estimated).

Contrary to the as-deposited sample, in the sample annealed at 600ºC for 1 hr the Ag layer is no longer located between two TiO_2 rich layers. The Ag has diffused towards the surface and the substrate/film interface. It seems, however, that there is less overall Ag in this sample, compared to the as-deposited one. The small 'dip' in the Ti signal shown in figure 9 cannot be explained by an increased local Ag concentration. Therefore this has arisen due to a locally increased concentration of Na (and possibly Ca), which could be explained by diffusion from the substrate. It seems that the diffusion of Na (and Ca) is preferentially towards the zone where Ag was originally present before annealing. Therefore, in this case, the local dip in the Ti concentration could be caused by agglomeration of Na arising from an ion-exchange diffusion

*Corresponding author: J.Kulczyk-Malecka@mmu.ac.uk
Tel: +441612476432

mechanism between Ag and Na ions, and hence the intensity of the diffused silver is significantly lower than in the as-deposited titania/Ag/titania sample.

4. Conclusions

In TiO_2/Ag/TiO_2 stacks, silver diffused at similar rates in the samples annealed at temperatures in the range of 100–400^{o}C, whereas a significant increase in diffusion coefficient was detected in the sample annealed at 600^{o}C for 5 minutes. This may be related to the structure of the titania layers, which showed a transformation from amorphous to anatase over this temperature range. Moreover, there could be a change in diffusion as a function of time, which would be related to the structure of deposited films and interfacial roughness.

Further investigations of silver diffusion in titania stacks showed that increasing the annealing time to 1 hour at 600^{o}C leads to complete loss of the silver layer, most likely into the glass substrate due to an ion-exchange mechanism. Sodium diffusion from the glass fills in the free spaces in the coatings created by the silver diffusion. Samples analysed by XPS have confirmed these results, as there was no silver detected in the stack after annealing at 600^{o}C for 1 hour. Also the RBS investigations confirmed the ion-exchange theory. However in the sample deposited onto a silicon wafer substrate, the silver diffused to the free surface creating large clusters on the film surface. EDX mapping analysis confirmed that the clusters were composed of silver. This implies that low-*E* glass toughening procedures applied at temperatures as high as 600^{o}C risk causing the diffusion of silver and sodium atoms into the neighbouring titania layers and may require the use of thin diffusion barrier layers.

*Corresponding author: J.Kulczyk-Malecka@mmu.ac.uk
Tel: +441612476432

Acknowledgments

Authors thank Dr. Mark Farnworth and Dr. Chris Wesbly from Pilkington Technology Management Ltd. for TOF-SIMS analysis and Dr. Vlad Vishnyakov from the Dalton Research Institute, MMU for SEM and EDX analysis.

References:

1. Ando E, Miyazaki M. *Thin Solid Films* 2001; 392: 289.
2. Glaser HJ. *Large Area Glass Coating*, 1st English ed. Germany: Von Ardenne Anglagentechnik GmbH; 2000.
3. Ando E, Suzuki S, Aomine N, Miyazaki M, Tada M. *Vacuum* 2000; 59: 792.
4. Chiba K, Takahashi T, Kageyama T, Oda H. *App. Surf. Sci.* 2005; 246: 48.
5. Hammarberg E, Roos A. *Thin Solid Films* 2003; 442: 222.
6. Kulczyk-Malecka J, Kelly PJ, West G, Clarke GCB, Ridealgh JA. *Thin Solid Films* 2011; 520: 1368.
7. Karunagaran B, Rajendra Kumar RT, Senthil Kumar V, Mangalaraj D, Narayandass SaK, Mohan Rao G. *Materials Science in Semiconductor Processing* 2003; 6: 547.
8. Karunagaran B, Kim K, Mangalaraj D, Yi J, Veluman S, *Solar Energy Materials & Solar Cells* 2005; 88: 199.
9. Pradhan SS, Sahoo S, Pradhan SK. *Thin Solid Films* 2010; 518: 6904.
10. Chung CK, Liao MW, Lai CW. *Thin Solid Films* 2009; 518: 1415.
11. Martinez-Morillas R, Sánchez-Marcos J, de Andrés A, Prieto C, *Surface & Coatings Technol*. 2010; 204: 1893.
12. Boukrouh S, Bensaha R, Bourgeois S, Finot E, Marco de Lucas MC. *Thin Solid Films* 2008; 516: 6353.

*Corresponding author: J.Kulczyk-Malecka@mmu.ac.uk
Tel: +441612476432

13. Tavares CJ, Vieira J, Rebouta L, Hungerford G, Coutinho P, Teixeira V, Carneiro JO, Fernandes AJ. *Materials Science and Engineering B* 2007; 138: 139.

14. Kelly PJ, Arnell RD. *Vacuum* 2000; 56: 159.

15. J. Kulczyk-Malecka, *"Diffusion Studies in Toughenable Low-E Coatings"*, PhD Thesis, School of Engineering, Manchester Metropolitan University, Manchester (2012).

16. Mayer M. *Nucl. Instr. and Meth. B* 2002; 194: 177.

17. Colaux JL, Demelenne L, Derycke I, Terwagne G. SIMTarget website, available from: http://www.fundp.ac.be/simtarget

18. Li Bassi A, Cattaneo D, Russo V, Bottani CE, Barborini E, Mazza T, Piseri P, Milani P, Ernst FO, Wegner K, Pratsinis SE. *J. Applied Physics* 2005; 98: 1.

19. Giolli C, Borgioli F, Credi A, Di Fabio A, Fossati A, Miranda MM, Parmeggiani S, Rizzi G, Scrivani A, Troglio S, Tolstoguzov A, Zoppi A, Bardi U. *Surface & Coatings Technology* 2007; 202: 13.

20. Sekiya T, Ohta S, Kamei S, Hanakawa M, Kurita S. J. *Physics and Chemistry of Solids* 2001;62: 717.

21. Khan AF, Mehmood M, Aslam M, Shah SI. *J. Colloid and Interface Science* 2010; 343: 271.

22. Balaji S, Djaoued Y, Robichaud J. *J. Raman Spectroscopy* 2006; 37: 1416.

23. Xie Y, Zhao X, Tao H, Zhao Q, Liu B, Yuan Q. *Chemical Physics Letters* 2008; 457: 148.

24. Crank J. *The Mathematics of Diffusion*, 2nd ed. Oxford: Clarendon Press; 1975.

*Corresponding author: J.Kulczyk-Malecka@mmu.ac.uk
Tel: +441612476432

25. Jackson KA. *Kinetic Processes. Crystal Growth, Diffusion, and Phase Transition in Materials.* Weinheim: WILEY-VCH; 2004.
26. Frank St, Södervall U, Herzig Chr. *Intermetallics* 1997; 5: 221.
27. Zulina NP, Bolberova EV, Rozumovskii IM. *Acta Mater.* 1996; 44: 3625.
28. Koskelo O, Räisänen J, Tuomisto F, Eversheim D, Grasza K, Mycielski A. *Thin Solid Films* 2010; 518: 3894.
29. Mallard WC, Gardner AB, Bass RF, Slifkin LM. *Physical Review* 1963; 129: 617.
30. Galindo RE, Gago R, Duday D, Palacio C. *Anal. Bioanal. Chem.* 2010; 396: 2725.
31. Hofmann S. *Phil. Trans. R. Soc. Lond. A* 2004; 362: 55.
32. Hofmann S. *Surf. Interface Anal.* 2000; 30: 228.
33. Zhang AY, Suetsugu T, Kadono K. *J. Non-Crystalline Solids* 2007; 353: 44.
34. Sheng J, Li J, Yu J. *International Journal of Hydrogen Energy* 2007; 32: 2598.
35. Prudenziati M, Morten B, Gualtieri AF, Leoni M. *J. Materials Science: Materials in Electronics* 2004; 15: 447.
36. Weast RC. *Handbook of Chemistry and Physics.* Cleveland, Ohio, USA: CRC Press Inc; 1974.

*Corresponding author: J.Kulczyk-Malecka@mmu.ac.uk
Tel: +441612476432

List of figure captions

Figure 1: Raman spectra of titania coatings on glass substrates from an as-deposited sample and samples annealed at 200 or 400ºC for 10 minutes, compared to rutile and anatase standards.

Figure 2: Raman spectra of titania coatings on glass substrates from samples annealed at 400 for 30 minutes or 600 ºC for 10 or 30 minutes, compared to anatase and rutile standards.

Figure 3: Arrhenius plot of silver diffusion coefficient in the range 100–600ºC, obtained from TiO_2/Ag/TiO_2 multilayer samples.

Figure 4: TOF-SIMS depth profiling collected from titania/silver/titania coating annealed at 600ºC for 1 hour (glass substrate).

Figure 5: XPS silver profiles from titania/silver/titania stacks deposited onto glass and silicon wafer substrates and annealed at 250 or 600ºC for 5 minutes or at 600ºC for 1 hour.

Figure 6: SEM image showing the surface morphology of titania/silver/titania samples deposited on float glass and annealed at a) 250ºC for 5 minutes, b) 600ºC for 1 hour; deposited on silicon wafer substrate and annealed at c) 250ºC for 5 minutes, d) 600ºC for 1 hr.

Figure 7: EDX mapping of TiO_2/Ag/TiO_2 sample deposited onto a Si wafer substrate. Comparing EDX results with the surface image (SEM), it can be seen that the white clusters agglomerated on the surface consists of silver atoms.

Figure 8: RBS spectrum from as-deposited titania/silver/titania sample on float glass substrate.

*Corresponding author: J.Kulczyk-Malecka@mmu.ac.uk
Tel: +441612476432

Figure 9: RBS spectrum from titania/silver/titania sample deposited onto float glass substrate and annealed at 600^{o}C for 1 hr.

Figure 10: Compositional depth profiles extracted from the RBS simulations. Elements were detected from coatings and a float glass substrate in the as-deposited titania/Ag/titania sample.

Figure 11: Silver concentration profiles from as-deposited and annealed titania/Ag/titania samples deposited onto a float-glass substrate. Profiles have been magnified to allow direct comparison between samples.

*Corresponding author: J.Kulczyk-Malecka@mmu.ac.uk
Tel: +441612476432

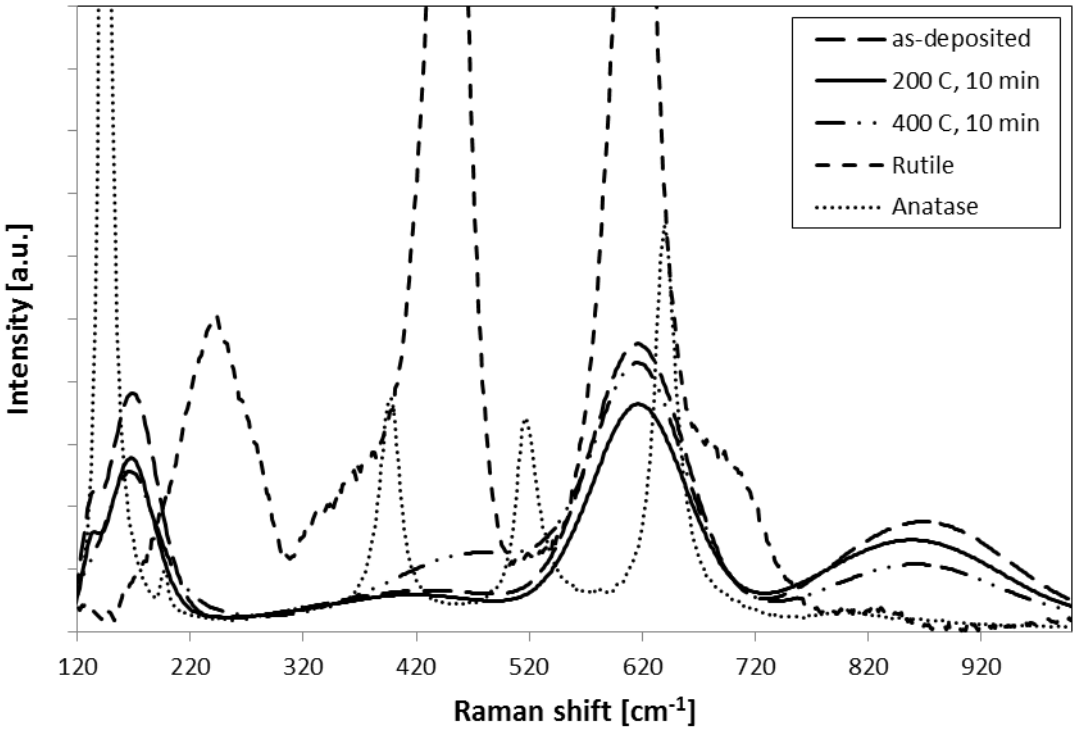

Figure 1

*Corresponding author: J.Kulczyk-Malecka@mmu.ac.uk
Tel: +441612476432

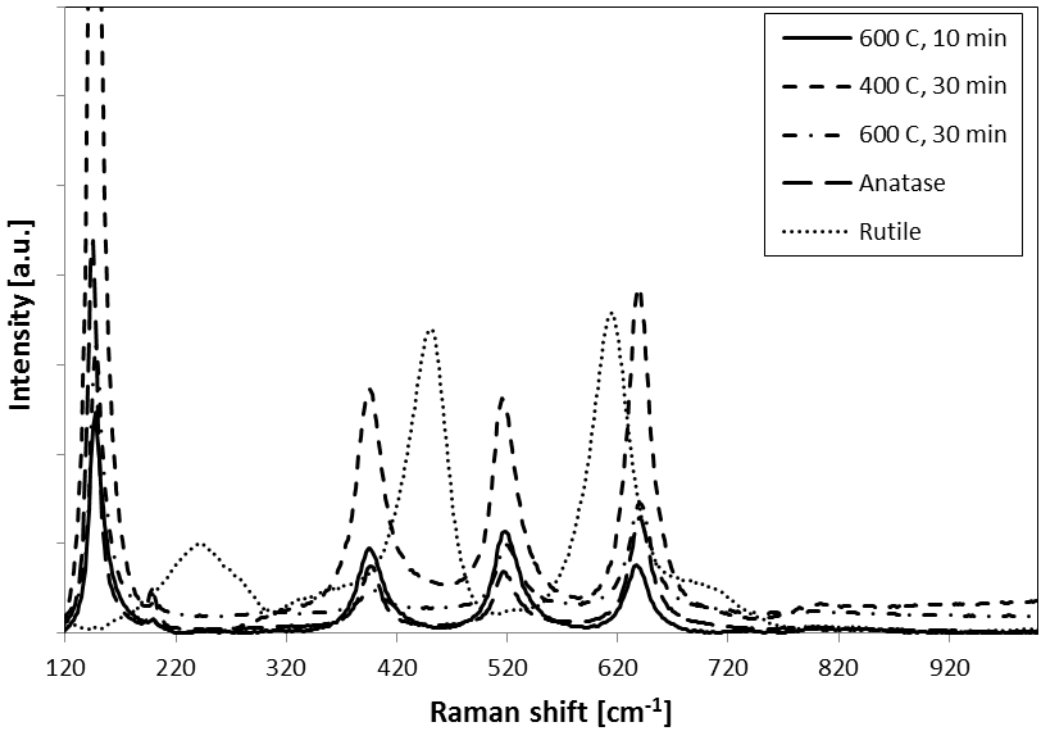

Figure 2

*Corresponding author: J.Kulczyk-Malecka@mmu.ac.uk
Tel: +441612476432

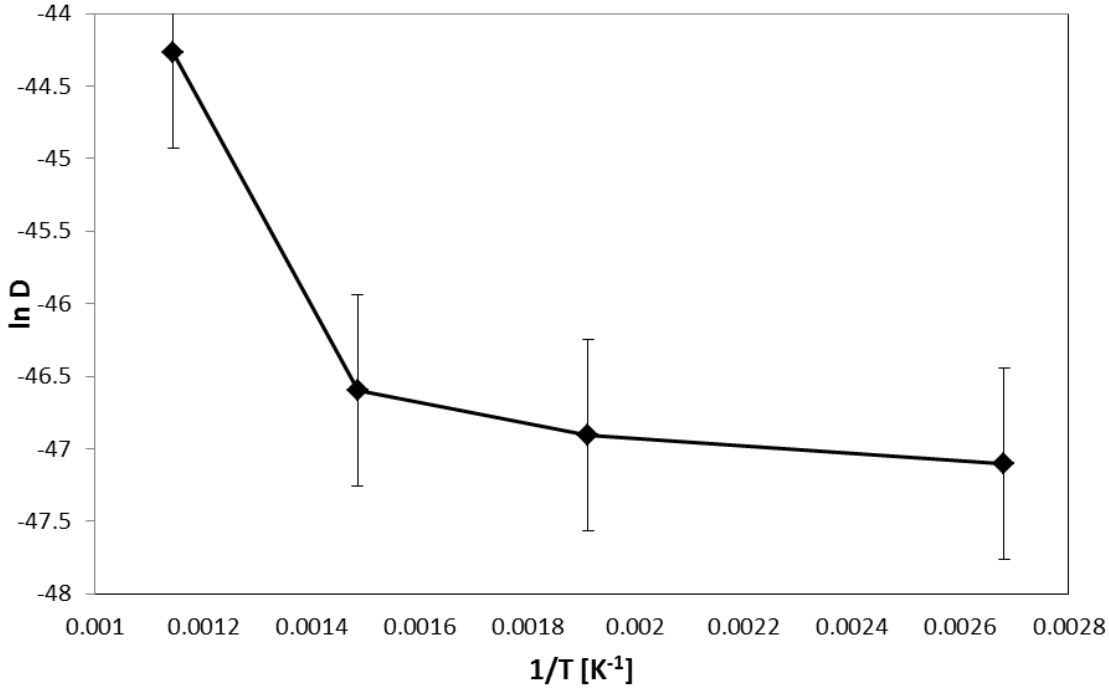

Figure 3

*Corresponding author: J.Kulczyk-Malecka@mmu.ac.uk
Tel: +441612476432

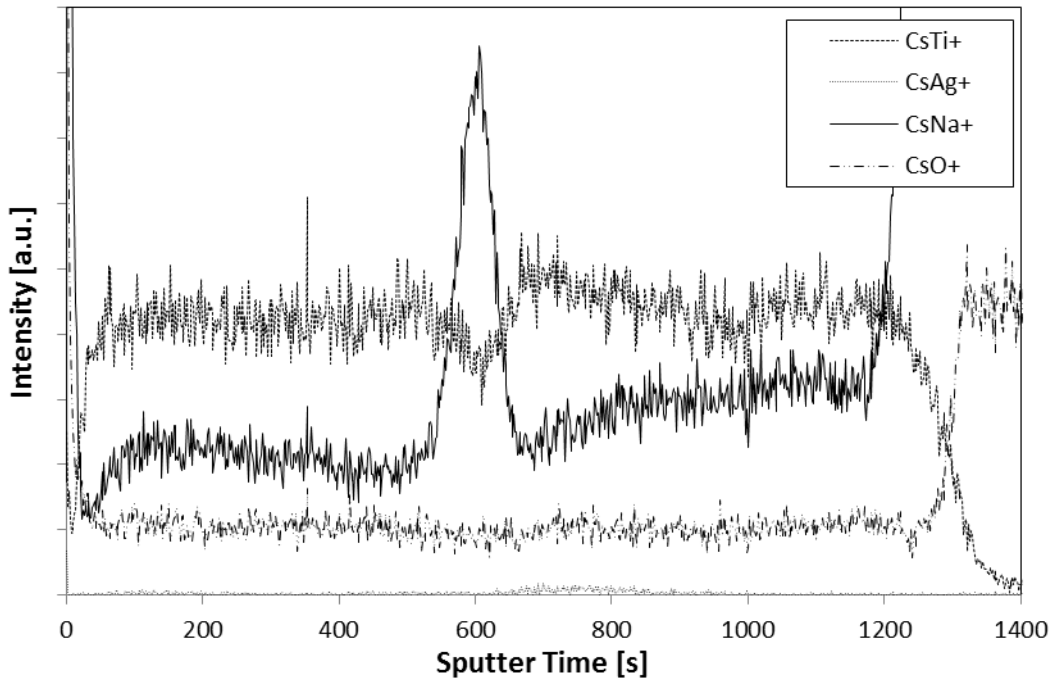

Figure 4

*Corresponding author: J.Kulczyk-Malecka@mmu.ac.uk
Tel: +441612476432

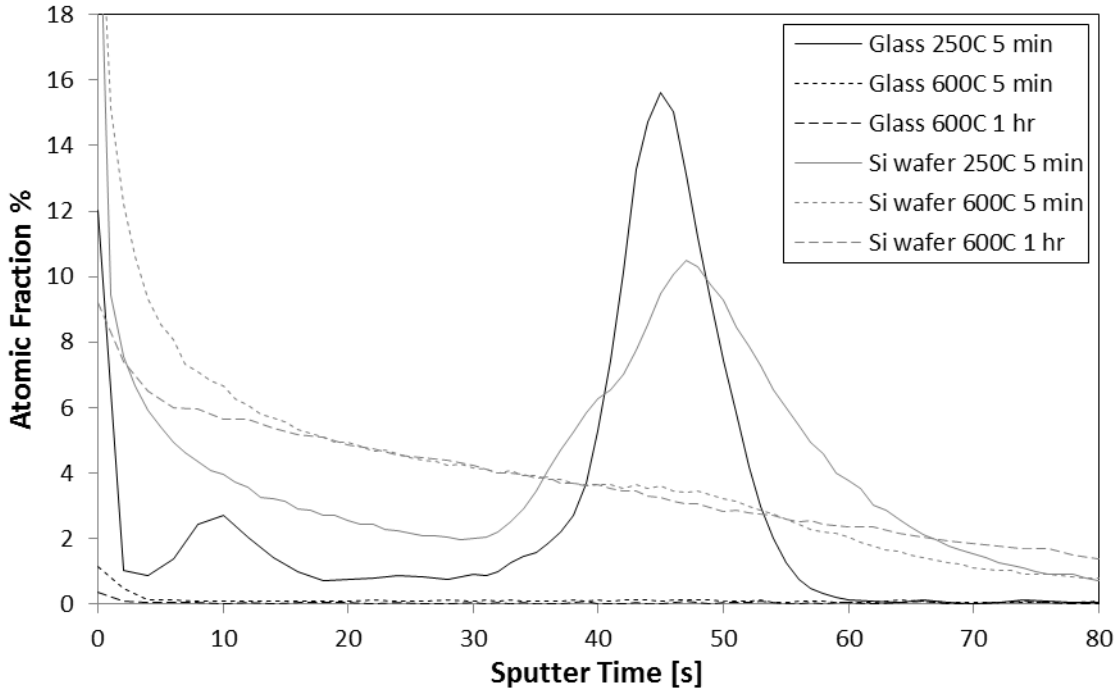

Figure 5

*Corresponding author: J.Kulczyk-Malecka@mmu.ac.uk
Tel: +441612476432

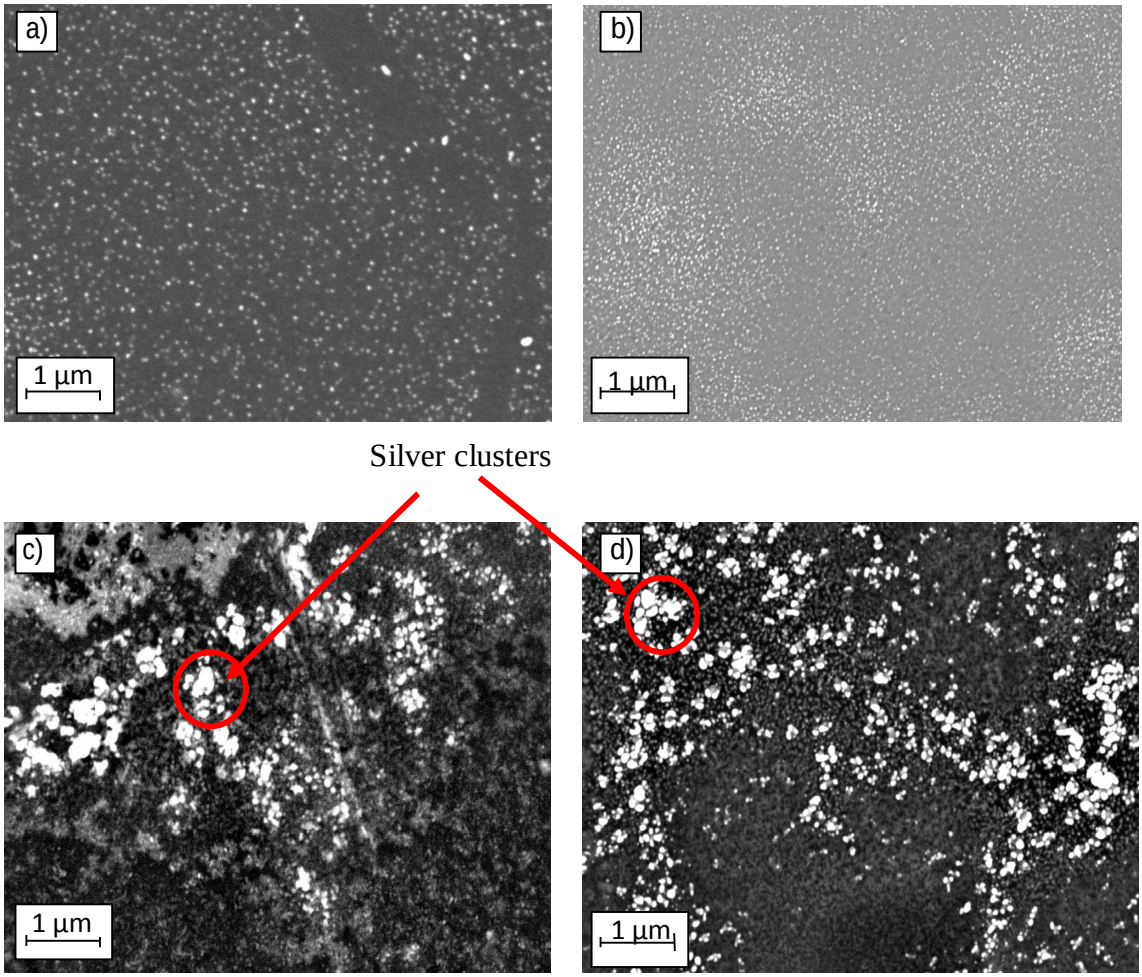

Figure 6

*Corresponding author: J.Kulczyk-Malecka@mmu.ac.uk
Tel: +441612476432

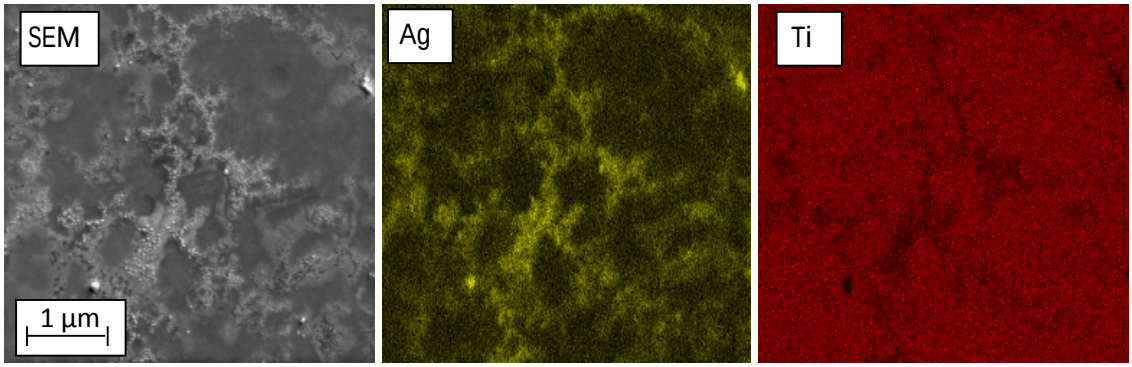

Figure 7

*Corresponding author: J.Kulczyk-Malecka@mmu.ac.uk
Tel: +441612476432

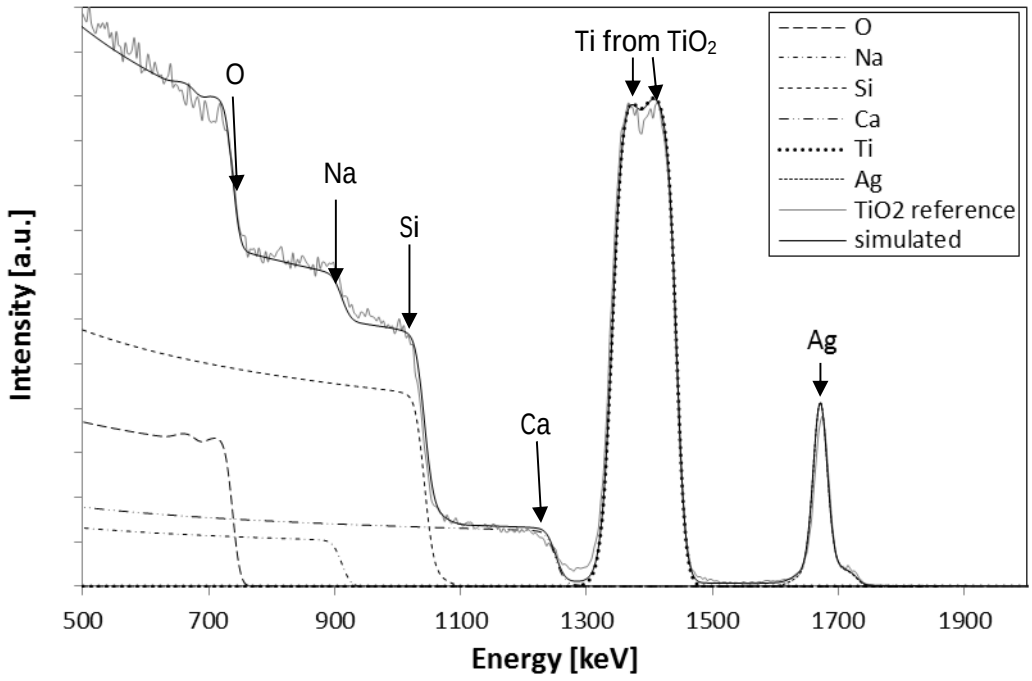

Figure 8

*Corresponding author: J.Kulczyk-Malecka@mmu.ac.uk
Tel: +441612476432

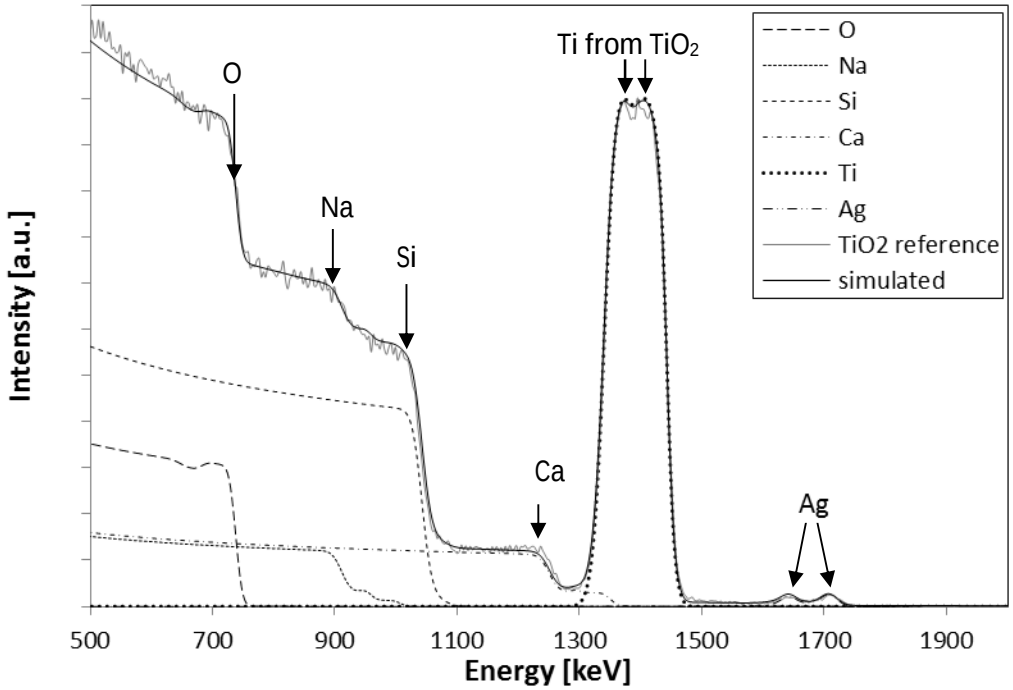

Figure 9

*Corresponding author: J.Kulczyk-Malecka@mmu.ac.uk
Tel: +441612476432

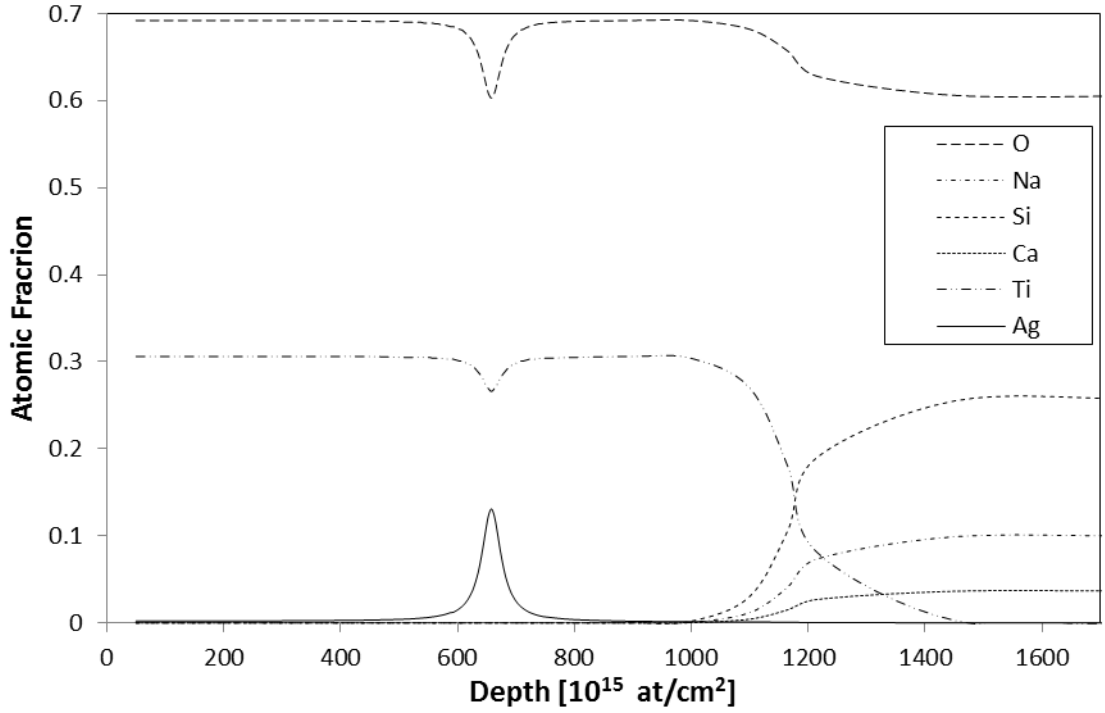

Figure 10

*Corresponding author: J.Kulczyk-Malecka@mmu.ac.uk
Tel: +441612476432

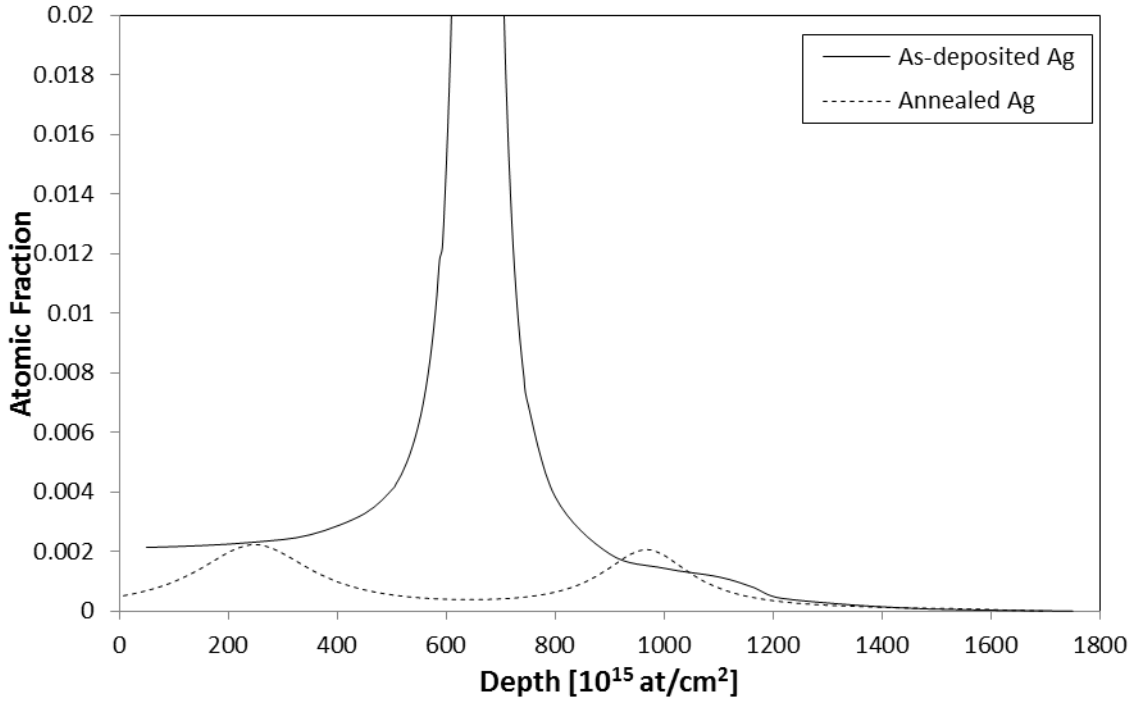

Figure 11

*Corresponding author: J.Kulczyk-Malecka@mmu.ac.uk
Tel: +441612476432

Table 1

Diffusion coefficient values calculated for $TiO_2/Ag/TiO_2$ stacks annealed over the temperature range of 100–600ºC for 5 minutes.

Annealing Temperature [ºC]	**Ag Diffusion Coefficient [m^2/s]**
100	$3.50x10^{-21}$
250	$4.25x10^{-21}$
400	$5.80x10^{-21}$
600	$5.93x10^{-20}$

*Corresponding author: J.Kulczyk-Malecka@mmu.ac.uk
Tel: +441612476432

Table 2

Elemental composition obtained from a $TiO_2/Ag/TiO_2$ stack deposited onto glass and annealed at 600^oC for 1 hour.

Element	Wt %	At %
O	38	54
Na	11	11
Mg	2	2
Al	3	3
Si	27	21
Ag	1	0.2
Ca	6	3
Ti	11	5

*Corresponding author: J.Kulczyk-Malecka@mmu.ac.uk
Tel: +441612476432

Table 3

Elemental composition obtained from a $TiO_2/Ag/TiO_2$ stack deposited onto Si wafer and annealed at 600^oC for 1 hour.

Element	Wt %	At %
O	15	27
Na	0.1	0.1
Si	60	62
Ag	12	3
Ti	13	8

*Corresponding author: J.Kulczyk-Malecka@mmu.ac.uk
Tel: +441612476432